

Synthesis of pyridoxal phosphate derivatives with antagonist activity at the P2Y₁₃ receptor

Yong-Chul Kim^a, Jung-Sun Lee^a, Katrin Sak^b,
Frederic Marteau^b, Liaman Mamedova^d,
Jean-Marie Boeynaems^{b,c}, Kenneth A. Jacobson^{d,*}

^aLaboratory of Drug Discovery, Department of Life Science, Gwangju Institute of Science and Technology, 1 Oryong-dong, Buk-gu, Gwangju 500-712, Republic of Korea

^bInstitute of Interdisciplinary Research, Free University of Brussels, Route de Lennik 808, Brussels 1070, Belgium

^cLaboratory of Medical Chemistry, Department of Clinical Pathology, Erasme Hospital, Route de Lennik 808, Brussels 1070, Belgium

^dMolecular Recognition Section, Laboratory of Bioorganic Chemistry, National Institute of Diabetes and Digestive and Kidney Diseases, National Institutes of Health, Bethesda, MD 20892-0810, USA

Received 26 January 2005; accepted 21 April 2005

Abstract

We have synthesized a series of derivatives of the known P2 receptor antagonist PPADS (pyridoxal-5'-phosphate-6-azo-phenyl-2,4-disulfonate) and examined their ability to inhibit functional activity of the recombinant human P2Y₁₃ nucleotide receptor expressed in 1321N1 human astrocytoma cells co-expressing Gα₁₆ protein (AG32). Analogues of PPADS modified through substitution of the phenylazo ring, including halo and nitro substitution, and 5'-alkyl phosphonate analogues were synthesized and tested. A 6-benzyl-5'-methyl phosphonate analogue was prepared to examine the effect of stable replacement of the azo linkage. The highest antagonistic potency was observed for 6-(3-nitrophenylazo) derivatives of pyridoxal-5'-phosphate. The 2-chloro-5-nitro analogue (MRS 2211) and 4-chloro-3-nitro analogue (MRS 2603) inhibited ADP (100 nM)-induced inositol trisphosphate (IP₃) formation with pIC₅₀ values of 5.97 and 6.18, respectively, being 45- and 74-fold more potent than PPADS. The antagonism of MRS 2211 was competitive with a pA₂ value of 6.3. MRS2211 and MRS2603 inhibited phospholipase C (PLC) responses to 30 nM 2-methylthio-ADP in human P2Y₁ receptor-mediated 1321N1 astrocytoma cells with IC₅₀ values of >10 and 0.245 μM, respectively. Both analogues were inactive (IC₅₀ > 10 μM) as antagonists of human P2Y₁₂ receptor-mediated PLC responses in 1321N1 astrocytoma cells. Thus, MRS2211 displayed >20-fold selectivity as antagonist of the P2Y₁₃ receptor in comparison to P2Y₁ and P2Y₁₂ receptors, while MRS2603 antagonized both P2Y₁ and P2Y₁₃ receptors. © 2005 Elsevier Inc. All rights reserved.

Keywords: PPADS (pyridoxal-5'-phosphate-6-azo-phenyl-2,4-disulfonate); Pyridoxal phosphate derivatives; Adenine nucleotides; P2Y₁₃ receptor; Inositol trisphosphate; Purines

1. Introduction

Extracellular nucleotides modulate cell functions via ionotropic P2X or G-protein-coupled P2Y receptors [1]. To date, eight human P2Y subtypes have been characterized. On the basis of phylogenetic relatedness they are divided into two distinct subgroups [2,3]. The first subgroup includes receptors for ADP (P2Y₁), ATP (P2Y₁₁), UTP (P2Y₄), UDP (P2Y₆) and a receptor for both ATP and UTP (P2Y₂). Within the second subgroup, P2Y₁₂ and P2Y₁₃ are ADP receptors, while P2Y₁₄ is activated by UDP-glucose and related sugar nucleotides.

Abbreviations: AG32, human astrocytoma 1321N1 cells co-expressing Gα₁₆ protein; AR-C67085MX, 2-(propylthio)-β,γ-dichloromethylene-ATP; CHO, Chinese Hamster ovary; DMEM, Dulbecco's Modified Eagle's Medium; FBS, fetal bovine serum; HRMS, high-resolution mass spectrometry; IP₃, inositol trisphosphate; KRH, Krebs-Ringer-HEPES; MRS 2211, pyridoxal-5'-phosphate-6-azo-(2-chloro-5-nitrophenyl)-2,4-disulfonate; MRS 2603, pyridoxal-5'-phosphate-6-azo-(4-chloro-3-nitrophenyl)-2,4-disulfonate; PLC, phospholipase C; PPADS, pyridoxal-5'-phosphate-6-azo-phenyl-2,4-disulfonate

* Corresponding author. Tel.: +1 301 496 9024; fax: +1 301 480 8422.

E-mail address: kajacobs@helix.nih.gov (K.A. Jacobson).

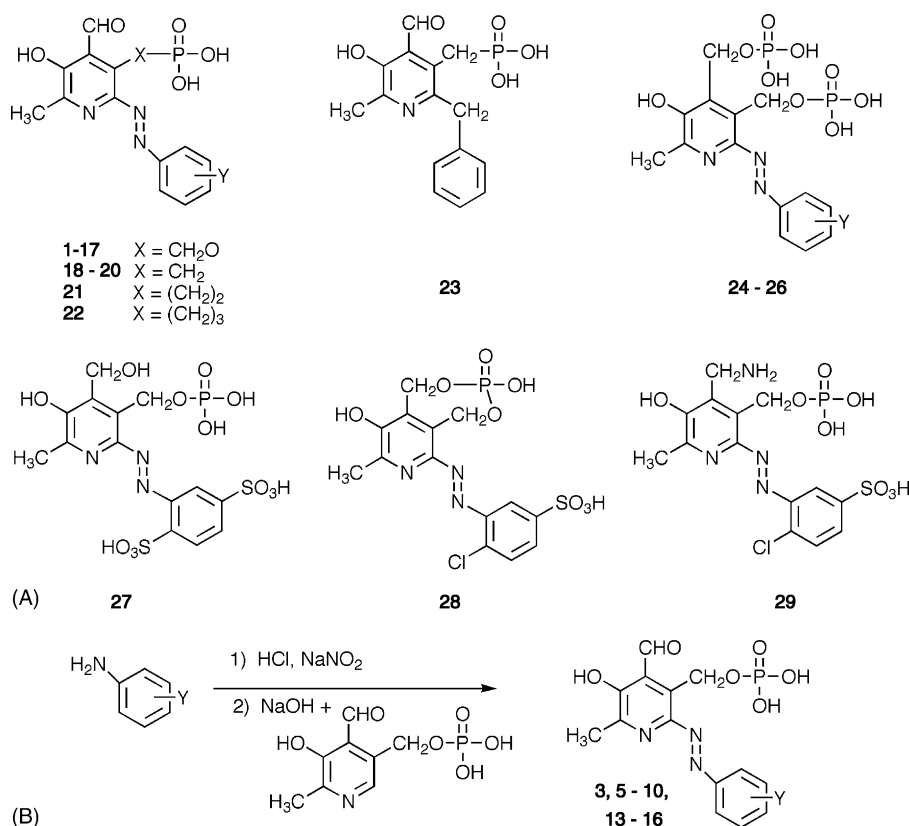


Fig. 1. Structures of pyridoxal phosphate derivatives tested in this study (A) and the synthetic method used to synthesize new analogues **3**, **5–10** and **13–16** (B). Substituents Y are defined in Table 1.

Selective antagonists are not yet available for most of these receptors. Pyridoxal-5'-phosphate-6-azophenyl-2',4'-disulfonate (PPADS, **1** in Fig. 1, Y = 2',4'-disulfonate) is a P2 receptor antagonist with 10–20-fold selectivity for P2X over P2Y receptors [4]. PPADS has been described as a competitive antagonist of the P2Y₁ receptor, having an inhibition constant around 10 μ M. It is inactive at P2Y₂ and P2Y₁₁ receptors and has only a slight inhibitory effect at high concentrations on P2Y₄ and P2Y₆ receptors [5,6]. Moreover, using a synthetic approach the antagonistic activity of PPADS at the P2Y₁ receptor has been slightly enhanced through the design of structural analogues, such as 6-(2'-chloro-phenylazo)-pyridoxal-5'-phosphate (MRS 2210) [7,8]. PPADS has been shown to have no effect on the P2Y₁₂ receptor [9–11]. However, despite the relatively high degree of amino acid identity (48%) between P2Y₁₂ and P2Y₁₃ receptors and their similar pharmacological profiles [12,13], PPADS was recently found to behave as a low potency antagonist for the P2Y₁₃ receptor with the inhibitory constant around 10 μ M [14].

We considered PPADS as a structural lead and have synthetically extended a previous series of analogues in an effort to identify more potent and/or selective P2Y₁₃ receptor antagonists. In the present study, we have tested a range of pyridoxal phosphate derivatives for inhibitory activity in a functional assay consisting of ADP-induced inositol trisphosphate synthesis in hP2Y₁₃-1321N1-G α ₁₆ cells.

2. Materials and methods

2.1. Chemical synthesis

Proton nuclear magnetic resonance spectroscopy was performed on a Bruker AVANCE 600, JEOL JNM-LA 300WB spectrometers and spectra were taken in DMSO-d₆. The chemical shifts are expressed as parts per million downfield from tetramethylsilane or as relative parts per million from HOD peaks (4.78 ppm). ³¹P NMR spectra were recorded at room temperature by use of Varian XL-300 spectrometer (121.42 MHz); orthophosphoric acid (85%) was used as an external standard. The identity of the purified products to be tested biologically was confirmed using high-resolution fast atom bombardment mass, performed on a JEOL SX102 spectrometer using 6-kV Xe atoms. The phosphate and phosphonate derivatives were desorbed from a matrix of glycerol or magic bullet. All pyridoxal phosphate and related phosphonate derivatives were homogeneous as judged by thin layer chromatography (Merck silica gel 60; F₂₅₄, 0.25 mm). The determinations of purity were performed with a Hewlett-Packard 1090 HPLC system using an OD-5-60 C18 analytical column (250 mm \times 4.6 mm, Separation Methods Technologies, Inc., Newark, DE) in two different linear gradient solvent systems. One solvent system (A) was 0.1 M triethylammonium acetate buffer: CH₃CN = 95:5 to

40:60 for 20 min with a flow rate of 1 ml/min. The other solvent system (B) was 5 mM tetrabutylammonium phosphate buffer:CH₃CN 80:20 to 40:60, in 20 min with a flow rate of 1 ml/min. Peaks were detected by ultraviolet absorption with a diode array detector.

2.1.1. General procedure of azo coupling for the synthesis of PPADS analogues

To a stirred solution of each aminoaryl compound (0.4 mmol) in 10 ml of water were added 0.4 ml (0.4 mmol) of 1 N HCl and 28 mg (0.4 mmol) of solid NaNO₂ at 0 °C. This solution was stirred for 5 min and the pH was adjusted to ~10 with 1 N NaOH (about 0.2 ml). To the mixture was added dropwise a solution of pyridoxal-5'-phosphate (100 mg, 0.4 mmol) previously dissolved in aqueous NaOH (pH ~10). The pH was adjusted to ~9, and the yellow color changed to red. After stirring for 30 min at 0 °C, the progress of reaction was monitored by HPLC using solvent system A. The product peaks appeared at retention times of 8–10 min with an ultraviolet absorption maximum at ~410 nm. The mixture was frozen and lyophilized, leaving a solid. The crude product was dissolved in a minimal volume of water and purified by ion-exchange column chromatography by using Amberlite CG-50 resin (H⁺ form, weakly acidic) and eluting with water (flow rate 0.5 ml/min). The red fraction showing a single peak in HPLC was collected and lyophilized to give the desired compounds (yield, 50–60%).

Starting with pyridoxal- α^5 -phosphate and the appropriate aryl amine and following the general procedure, we have synthesized compounds **3**, **5–10** and **13–16** (Table 1). Other pyridoxal phosphate derivatives were prepared as reported [7,15,16].

2.1.2. Pyridoxal-5'-phosphate-6-azo-(2-fluorophenyl)-2,4-disulfonate (**3**)

Yield = 65%. ¹H NMR (DMSO-d₆) δ 2.34 (3H, s, -CH₃), 5.66 (2H, d, J = 5.1 Hz, -CH₂O), 7.23 (1H, t, J = 7.8 Hz, phenyl), 7.52 (1H, d, J = 8.4 Hz, phenyl), 7.76 (1H, t, J = 7.8 Hz, phenyl), 7.85 (1H, d, J = 8.4 Hz, phenyl), 10.42 (1H, s, CHO).

2.1.3. Pyridoxal-5'-phosphate-6-azo-(2-bromophenyl)-2,4-disulfonate (**5**)

Yield = 68%. ¹H NMR (DMSO-d₆) δ 2.36 (3H, s, -CH₃), 5.65 (2H, d, J = 5.1 Hz, -CH₂O), 7.30 (1H, t, J = 7.6 Hz, phenyl), 7.40 (1H, t, J = 7.6 Hz, phenyl), 7.66 (1H, d, J = 7.8 Hz, phenyl), 7.75 (1H, d, J = 7.8 Hz, phenyl), 10.41 (1H, s, CHO).

2.1.4. Pyridoxal-5'-phosphate-6-azo-(2-iodophenyl)-2,4-disulfonate (**6**)

Yield = 50%. ¹H NMR (DMSO-d₆) δ 2.36 (3H, s, -CH₃), 5.65 (2H, d, J = 5.4 Hz, -CH₂O-), 7.16 (1H, t, J = 7.5 Hz, phenyl), 7.40 (1H, t, J = 7.5 Hz, phenyl), 7.55 (1H, d, J = 8.0 Hz, phenyl), 8.01 (1H, d, J = 8.0 Hz, phenyl), 10.42 (1H, s, CHO).

2.1.5. Pyridoxal-5'-phosphate-6-azo-(3-chlorophenyl)-2,4-disulfonate (**7**)

Yield = 76%. ¹H NMR (DMSO-d₆) δ 2.29 (3H, s, -CH₃), 5.64 (2H, d, J = 4.8 Hz, -CH₂O-), 7.42 (1H, d, J = 8.1 Hz, phenyl), 7.48 (1H, t, J = 7.8 Hz, phenyl), 7.80 (1H, d, J = 8.1 Hz, phenyl), 7.81 (1H, s, phenyl), 10.39 (1H, s, CHO).

Table 1
Antagonism of human P2Y₁₃ receptors by pyridoxal derivatives

Compound		Substitution ^a		Percent of inhibition at 10 μ M (%)	Potency (pIC ₅₀)
		X	Y		
1	PPADS	CH ₂ O	2,4-(SO ₃ H) ₂	13.3	4.31 \pm 0.51
2	isoPPADS	CH ₂ O	2,5-(SO ₃ H) ₂	32.1	4.73 \pm 0.22
3		CH ₂ O	2-F	70.3	5.53 \pm 0.09
4	MRS2210	CH ₂ O	2-Cl	70.6	5.21 \pm 0.16
5		CH ₂ O	2-Br	67.7	5.59 \pm 0.17
6		CH ₂ O	2-I	67.3	5.32 \pm 0.15
7		CH ₂ O	3-Cl	75.4	5.62 \pm 0.15
8		CH ₂ O	4-Cl	52.9	5.52 \pm 0.22
9		CH ₂ O	3-F	65.6	5.68 \pm 0.15
10	MRS2592	CH ₂ O	3-NO ₂	77.5	5.76 \pm 0.20
11		CH ₂ O	2-Cl-5-SO ₃ H	70.1	5.31 \pm 0.19
12	MRS2211	CH ₂ O	2-Cl-5-NO ₂	83.8	5.97 \pm 0.04
13	MRS2603	CH ₂ O	4-Cl-3-NO ₂	85.3	6.18 \pm 0.10
14		CH ₂ O	2,4-F ₂	64.9	5.51 \pm 0.18
15		CH ₂ O	2,3,4-F ₃	26.8	4.32 \pm 0.16
16		CH ₂ O	4-F-3-NO ₂	44.0	5.06 \pm 0.33
19		CH ₂	2-Cl-5-SO ₃ H	60.7	5.21 \pm 0.15

Inositol trisphosphate responses were measured by pre-incubating the hP2Y₁₃-AG32 cells with PPADS derivatives for 10 min and then stimulating with 100 nM ADP for 30 s. Values are mean \pm S.E.M.

^a Structures are given in Fig. 1. Compounds (Y=) **17** (3-Cl-4-CO₂H), **21** and **22** (2-Cl-5-SO₃H), **23**, **25** (2,5-di-SO₃H), **26** (2-Cl-5-SO₃H), and **29** weakly inhibited (30–46%) at 10 μ M. Compound **18** (2,5-di-SO₃H), **20** (3,5-di-CH₂PO₃H₂), and **24** (H) at 10 μ M inhibited by 67.8%, 72.1%, and 51.1%, respectively, however, IC₅₀ values were not determined. Compounds **27** and **28** showed no inhibition at 10 μ M.

2.1.6. *Pyridoxal-5'-phosphate-6-azo-(4-chlorophenyl)-2,4-disulfonate (8)*

Yield = 48%. ¹H NMR (DMSO-d₆) δ 2.32 (3H, s, -CH₃), 5.62 (2H, d, *J* = 5.1 Hz, -CH₂O-), 7.49 (2H, d, *J* = 8.4 Hz, phenyl), 7.84 (2H, d, *J* = 8.4 Hz, phenyl), 10.40 (1H, s, CHO).

2.1.7. *Pyridoxal-5'-phosphate-6-azo-(3-fluorophenyl)-2,4-disulfonate (9)*

Yield = 87%. ¹H NMR (D₂O) δ 2.47 (3H, s, -CH₃), 5.68 (2H, d, *J* = 4.5 Hz, -CH₂O-), 7.24 (1H, pseudo t, *J* = 7.8 Hz, *J* = 8.4 Hz phenyl), 7.48 (1H, s, phenyl), 7.51 (1H, d, *J* = 8.4 Hz, phenyl), 7.66 (1H, d, *J* = 7.8 Hz, phenyl), 10.42 (1H, s, CHO).

2.1.8. *Pyridoxal-5'-phosphate-6-azo-(3-nitrophenyl)-2,4-disulfonate (10)*

Yield = 30%. ¹H NMR (D₂O) δ 2.45 (3H, s, -CH₃), 5.69 (2H, d, *J* = 4.4 Hz, -CH₂O-), 7.72 (1H, t, *J* = 8.0 Hz, phenyl), 8.20 (1H, d, *J* = 8.0 Hz, phenyl), 8.25 (1H, d, *J* = 8.0 Hz, phenyl), 8.48 (1H, s, phenyl), 10.41 (1H, s, CHO).

2.1.9. *Pyridoxal-5'-phosphate-6-azo-(4-chloro-3-nitrophenyl)-2,4-disulfonate (13)*

Yield = 25%. ¹H NMR (D₂O) δ 2.39 (3H, s, -CH₃), 5.65 (2H, d, *J* = 5.4 Hz, -CH₂O-), 7.74 (1H, d, *J* = 9.3 Hz, phenyl), 8.10 (1H, d, *J* = 9.3 Hz, phenyl), 8.39 (1H, s, phenyl), 10.39 (1H, s, CHO). HRMS (FAB-) calcd.: 429.0003; found: 428.9980.

2.1.10. *Pyridoxal-5'-phosphate-6-azo-(2,4-difluorophenyl)-2,4-disulfonate (14)*

Yield = 26%. ¹H NMR (D₂O) δ 2.49 (3H, s, -CH₃), 5.73 (2H, d, *J* = 3.3 Hz, -CH₂O-), 7.07 (1H, d, *J* = 6.6 Hz, phenyl), 7.17 (1H, pseudo t, *J* = 9.0 Hz, *J* = 9.6 Hz, phenyl), 7.93 (1H, d, *J* = 6.6 Hz, phenyl), 10.46 (1H, s, CHO).

2.1.11. *Pyridoxal-5'-phosphate-6-azo-(2,3,4-trifluorophenyl)-2,4-disulfonate (15)*

Yield = 31%. ¹H NMR (D₂O) δ 2.50 (3H, s, -CH₃), 5.22 (2H, d, *J* = 6.9 Hz, -CH₂O-), 6.48 (1H, m, phenyl), 7.50 (1H, m, phenyl), 10.44 (1H, s, CHO).

2.1.12. *Pyridoxal-5'-phosphate-6-azo-(4-fluoro-3-nitrophenyl)-2,4-disulfonate (16)*

Yield = 86%. ¹H NMR (D₂O) δ 2.52 (3H, s, -CH₃), 5.22 (2H, d, *J* = 6.78 Hz, -CH₂O-), 6.51 (1H, d, *J* = 7.2 Hz, phenyl), 7.52 (1H, s, phenyl), 7.78 (1H, d, *J* = 7.2 Hz, phenyl), 10.46 (1H, s, CHO).

2.1.13. *Synthesis of the 6-benzyl analogue of PPADS (23)*

The general scheme of synthesis is described in Section 3.

2.1.13.1. *6-(Benzyl)pyridoxal-4-dimethylacetal (32)*. 3-Trimethylcarbonyl-6-(benzyl)pyridoxal monomethylacetal (**30**) (0.77 g, 2.16 mmol), prepared as described [17], was treated with a solution of 10% sulphuric acid (2 ml) in acetone (4 ml) and heated at 48 °C for 48 h. Workup with ether/saturated sodium bicarbonate followed by silica column chromatography eluting with CHCl₃:MeOH (150:1) yielded **31** (0.52 g, 79%). ¹H NMR (CDCl₃) δ 1.38 (9H, s, *t*-Bu), 2.44 (3H, s, -CH₃), 3.64 (d, OH, *J* = 7.81 Hz), 4.07 (2H, s, -CH₂-), 4.74 (2H, dd, *J* = 12.7 Hz, *J* = 58.6 Hz, CH₂O-), 5.93 (1H, s, -CH-), 7.16–7.28 (5H, m, phenyl). MS (Cl, NH₃) 342 (*M* + H).

Compound **31** (150 mg, 0.439 mmol) was dissolved in 1 ml of 10% methanolic potassium hydroxide solution and the mixture was allowed to stand for 10 min. The mixture was cooled in an ice bath, and 1 equivalent of acetic acid was added for neutralisation. The product was purified by preparative thin layer chromatography with CHCl₃:MeOH (20:1) and crystallized from hexane:ethyl acetate (10:1) to afford 90 mg of **31** as a white solid (yield 68%). ¹H NMR (CDCl₃) δ 2.50 (3H, s, -CH₃), 3.44 (6H, s, 2*x*-OCH₃), 4.25 (2H, s, -CH₂-), 4.59 (2H, s, -CH₂-), 5.93 (1H, s, -CH-), 7.16–7.29 (5H, m, phenyl), 8.73 (1H, s, -OH). MS (Cl, NH₃) 304 (*M* + H).

2.1.13.2. *Dimethyl[4-formyl-3-hydroxy-2-methyl-6-benzyl-pyrid-5-yl]methylphosphonate (33)*. Compound **32** (80 mg, 0.263 mmol) was treated with 0.5 ml of thionyl chloride and the mixture was stirred for 5 min. The excess thionyl chloride was removed by a N₂ stream and reduced pressure. The residue was dissolved in anhydrous CH₂Cl₂, neutralized with triethylamine and filtered through a bed of silica gel eluting with CHCl₃/MeOH (100/1). After evaporation, 85 mg of the chloromethyl compound was obtained (100%). ¹H NMR (CDCl₃) δ 2.50 (3H, s, -CH₃), 3.44 (6H, s, 2*x*-OCH₃), 4.25 (2H, s, -CH₂-), 4.55 (2H, s, -CH₂-), 5.86 (1H, s, -CH-), 7.17–7.29 (5H, m, phenyl), 8.81 (1H, s, -OH). HRMS (EI) calcd.: 321.1132; found 321.1129.

The chloromethyl compound was dissolved in 1 ml of trimethylphosphite, and heated at 65 °C for 2 days and 70 °C for 1 day. After evaporation of the excess trimethylphosphite, the residue was purified by preparative thin layer chromatography with CHCl₃:MeOH (20:1) to afford 30 mg of **33** as a light yellow oil with recovery of 20 mg of the starting compound (combined yield 38%). ¹H NMR (CDCl₃) δ 2.48 (3H, d, *J* = 2.6 Hz, -CH₃), 3.16 (2H, d, *J* = 21.6 Hz, -CH₂P-), 3.43 (6H, s, 2*x*-OCH₃), 3.68 (6H, d, *J* = 11.0 Hz, -P(O)(OCH₃)₂), 4.28 (2H, s, -CH₂-), 6.16 (1H, s, -CH-), 7.09–7.28 (5H, m, phenyl), 9.01 (1H, s, -OH). ³¹P NMR (CDCl₃) 28.76 (m). MS (Cl, NH₃) 396 (*M* + H).

2.1.13.3. *[4-Formyl-3-hydroxy-2-methyl-6-benzyl-pyrid-5-yl]methylphosphonic acid monotriethylamine salt (23)*. A solution of 50 mg (0.126 mmol) of **33** in 3 ml of anhydrous CH₂Cl₂ was treated with 70 μl (0.5 mmol) of bromotrimethylsilane at 25 °C. The mixture was stirred

overnight and partitioned between water and CH_2Cl_2 . The aqueous layer was evaporated and purified by C18 low pressure column chromatography using HPLC solvent system A. Pure fractions were combined, evaporated and repeated lyophilization afforded 26 mg of **23** as yellow solid (64%). ^1H NMR (D_2O) δ 1.22 (9H, t, $J = 7.3$ Hz, $3x\text{-CH}_3$), 2.40 (3H, s, $-\text{CH}_3$), 3.13 (6H, q, $J = 7.3$ Hz, $3x\text{-CH}_2$), 3.20 (2H, d, $J = 21.8$ Hz, $-\text{CH}_2\text{P}-$), 4.25 (2H, s, $-\text{CH}_2-$), 7.12 (2H, d, $J = 7.8$ Hz, phenyl), 7.18–7.28 (3H, m, phenyl), 9.99 (1H, s, $-\text{CHO}$). ^{31}P NMR (D_2O) 15.98 (t, $J = 21.8$ Hz). HRMS (FAB $^-$) calcd.: 320.0688, found: 320.0689. HPLC retention time 11.2 min (purity >98%), min (>98% purity) using solvent system B.

2.2. Cell culture

Previously constructed human astrocytoma 1321N1 cells expressing $\text{G}\alpha_{16}$ protein and stably transfected with hP2Y₁₃ receptors (hP2Y₁₃-1321N1- $\text{G}\alpha_{16}$) [12] were used. Cells were cultured in Dulbecco's Modified Eagle's Medium (DMEM) (Gibco) supplemented with 10% of fetal bovine serum (FBS; v/v), 100 units/ml of penicillin, 100 $\mu\text{g}/\text{ml}$ of streptomycin, 400 $\mu\text{g}/\text{ml}$ of G418, and 500 $\mu\text{g}/\text{ml}$ of zeocin. Cells were grown at 37 °C in a humidified atmosphere of 95% air and 5% CO_2 in 9-cm Petri dishes.

2.3. Inositol trisphosphate (IP_3) assay

Formation of inositol trisphosphate was measured as described in [14]. Briefly, the hP2Y₁₃-AG32 cells (200,000 cells/well) were seeded on 35-mm diameter cell culture dishes in complete medium two days before the experiment. One day before the experiment the incubation medium was changed by DMEM supplemented with 5% of FBS (v/v), antibiotics, G418, and [*myo*-D-2- ^3H]-inositol (5 $\mu\text{Ci}/\text{ml}$). After 18 h this labelling medium was aspirated and the cells were incubated in Krebs–Ringer–HEPES (KRH) buffer (124 mM NaCl, 5 mM KCl, 1.25 mM MgSO_4 , 1.45 mM CaCl_2 , 1.25 mM KH_2PO_4 , 25 mM HEPES, pH 7.4, and 8 mM D-glucose) for 2 additional hours. The cells were then pre-treated with antagonist solutions or buffer alone for 10 min at 37 °C followed by the addition of ADP for 30 s. Reactions were terminated upon aspiration of the medium and addition of 1 ml of 3% ice-cold perchloric acid solution. Inositol trisphosphate was then separated on Dowex columns as described previously [18]. Inhibition of phospholipase C (PLC) responses to 2-methylthio-ADP in human P2Y₁ receptor-expressing 1321N1 cells was measured as reported [8], and similar methods were used for human P2Y₁₂ receptor-mediated responses.

2.4. Reagents

ADP was obtained from Sigma Chemicals (St. Louis, MO), PPADS and isoPPADS were from Tocris (Bristol,

UK). Formic acid (HCOOH) and perchloric acid (HClO_4) were purchased from Merck. Ammonium formate was obtained from the BDH Laboratory. Radioactive product [*myo*-D-2- ^3H]-inositol was from Amersham Biosciences (Piscataway, NJ). Dowex AG1-X8 resin (formate form) was a product of Bio-Rad Laboratories (Hercules, CA).

2.5. Data analysis

IC_{50} values were derived from inhibition curves fitted to the data by logistic, nonlinear regression analysis using the GraphPad Prism 4.00 Software (San Diego, CA, USA).

3. Results

3.1. Design of pyridoxal phosphate derivatives as potential antagonists for the P2Y₁₃ receptor

The structure of the P2 antagonist PPADS (**1**) is provided in Table 1 and Fig. 1. There is an arylsulfonate group coupled to a pyridoxal phosphate moiety through an azo linkage. A positional isomer, “isoPPADS” (**2**), was found to be slightly more potent than PPADS as an antagonist of P2X₁ receptors [15]. We have examined the P2Y₁₃ receptor potency of PPADS, isoPPADS, and analogues of PPADS (Fig. 1A) modified through substitution of the phenylazo ring, including mono-halo substitution (**3–9**), nitro substitution (**10**), and combinations of the above (**11–17**). Also, methyl- (**18–20**), ethyl- (**21**), and propyl- (**22**) phosphonate analogues previously prepared [7,15] were examined as P2Y₁₃ receptor antagonists. The 6-benzyl analogue **23** (also a methylphosphonate) [16], was prepared to examine the effects on P2 receptor interaction of carbon (stable) replacement of the azo linkage. Replacement of the 4-aldehyde group with hydroxymethyl (**27**), a second phosphate moiety **24–26**, a cyclic phosphate (**28**), and aminomethyl (**29**) was also included.

Compounds **3**, **5–10**, and **13–16** were synthesized using a standard method of amine diazotization and coupling to pyridoxal phosphate (Fig. 1B), and the synthesis scheme of analogue **23** is depicted in Fig. 2. The starting cyclic acetal **30** was prepared as described [17] and was treated successively with acetone/sulphuric acid and potassium hydroxide/methanol to give the dimethylacetal **32**. The free hydroxymethyl group was converted to chloromethyl and then phosphorylated by an Arbuzov reaction to give **33**. Deprotection using trimethylsilyl bromide provided the free phosphonate **23**.

3.2. Antagonistic effect of pyridoxal phosphate derivatives on ADP-induced IP_3 synthesis in hP2Y₁₃-1321N1 cells co-expressing $\text{G}\alpha_{16}$ protein

Activation of PLC was examined as the functional assay of antagonism of the P2Y₁₃ nucleotide receptor. The

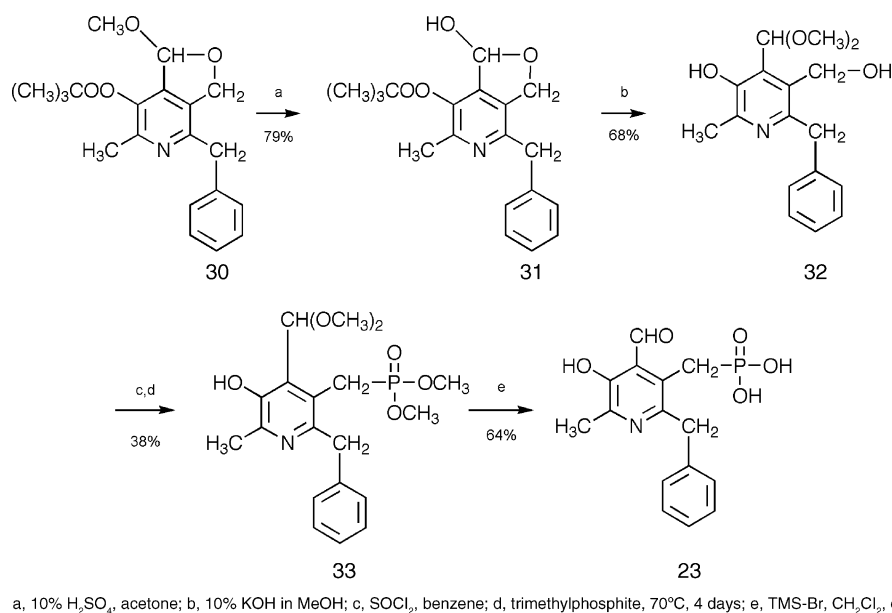


Fig. 2. Scheme used for the synthesis of the 6-benzyl analogue of PPADS (**23**). Reagents: (a) 10% sulfuric acid in acetone; (b) 10% potassium hydroxide in methanol; (c) thionyl chloride in benzene; (d) trimethylphosphite, 70 °C, 4 days; and (e) trimethylsilyl bromide in methylene chloride, overnight.

recombinant human P2Y₁₃ nucleotide receptor was expressed in engineered 1321N1 human astrocytes (AG32 cells co-expressing G α ₁₆ protein). G α ₁₆ protein is used as an adaptor protein to allow a variety of GPCRs, such as the normally G_i-coupled P2Y₁₃ receptor, to signal through PLC- β [22]. Initially, the compounds were tested at a single concentration (10 μ M) as inhibitors of PLC activity induced by 100 nM ADP, and the more potent analogues were characterized by full concentration–response curves. These data are listed in Table 1.

A positional isomer “isoPPADS” (**2**) was a slightly more potent antagonist than PPADS (**1**), with a pIC₅₀ value of 4.73 as compared to 4.31 (Fig. 3).

In the series of mono halo-substituted analogues, the lowest potency was observed for the 2-iodo derivative **6**. The effects of the position of chloro substitution were tested in analogues **4**, **7**, and **8**. The potencies were not significantly different, however, the *m*-substitution of **7** provided a pIC₅₀ value of 5.62, which represents a 20-fold gain in potency over PPADS. A *m*-fluoro derivative **9** was equipotent to **7**.

The most potent antagonists among the present series of pyridoxal phosphate derivatives in the PLC assay were the 3-nitro (**10**, MRS 2592), the 2-Cl-5-nitro (**12**, MRS 2211), and the 4-Cl-3-nitro (**13**, MRS 2603) analogues, with pIC₅₀ values of 5.76, 5.97, and 6.18, respectively. Compounds **13** and **12** were 74- and 45-fold more potent than PPADS (Fig. 3). Compound **12** was shown by Schild analysis to behave as a competitive antagonist with pA₂ value of 6.3 \pm 0.1 and a slope of approximately unity (Fig. 4). Since the PPADS derivatives were added 10 min prior to ADP addition, it was checked that inhibition by compound **12** did not result from transient stimulation followed by desensitization (data not shown). All these analogues (**10**,

12, **13**) contained the *m*-nitro group. Compound **12** was significantly more potent than the corresponding analogue **11**, in which the nitro group was replaced with a sulfonate group. The 4-fluoro-3-nitro analogue **16** was significantly less potent than the corresponding 4-chloro analogue **12**.

The potencies of the phosphonate derivatives indicated that the methylphosphonates were comparable to the methoxy derivatives (PPADS-like) as P2Y₁₃ antagonists: e.g. for the 2-chloro-5-sulfonate analogues, the IC₅₀ of **19** was 6 μ M as compared to 5 μ M for compound **11**. Although complete inhibition curves were not obtained,

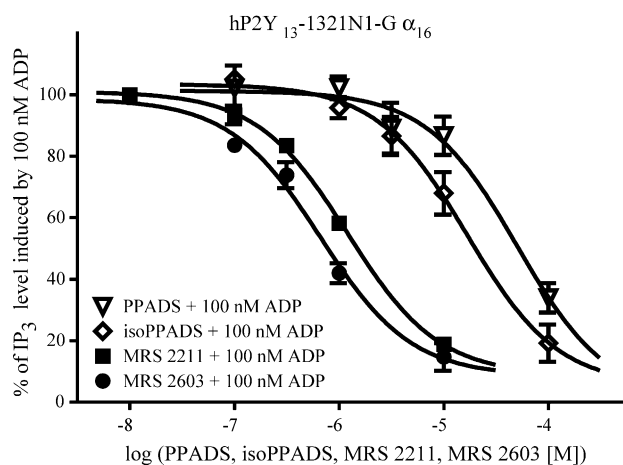


Fig. 3. Antagonistic effect of compounds **12** and **13** on IP₃ synthesis induced by 100 nM ADP. After overnight labelling of hP2Y₁₃-1321N1-G α ₁₆ with [*myo*-D-2-³H]-inositol, the cells were pre-incubated with various concentrations of PPADS, isoPPADS, analogues **12** (MRS 2211) and **13** (MRS 2603) or buffer alone for 10 min followed by addition of 100 nM ADP for 30 s. Formation of IP₃ was measured as described in Section 2. The data are expressed as mean \pm S.E.M. of one representative experiment done in duplicate. The IC₅₀ values are listed in Table 1.

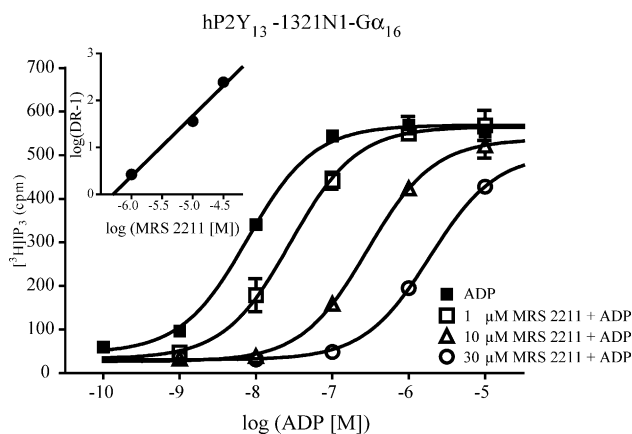


Fig. 4. Inhibitory effect of analogue **12** on ADP-induced IP₃ synthesis measured in hP2Y₁₃-1321N1-Gα₁₆. The cells were pre-treated with compound **12** (MRS 2211) or buffer alone for 10 min and then various concentrations of ADP were added for 30 s. The inset shows the Schild plot of the data with the X-intercept (pA₂) of 6.3 ± 0.1 and slope of 1.3 ± 0.1. IP₃ was quantified as described in Section 2. The data are presented as mean ± S.E.M. of one representative experiment done in duplicate.

the percent inhibition at 10 μM of the longer ethyl **21** and propyl **22** phosphonates indicated lower potency (<50% inhibition at 10 μM, data not shown). The 6-benzyl analogue **23** (also a methylphosphonate) [16], the bisphosphates **24–26**, and the aminomethyl analogue **29** at 10 μM were weak antagonists of the P2Y₁₃ receptor-mediated PLC response (≤50% inhibition at 10 μM, data not shown). Replacement of the 4-aldehyde group with hydroxymethyl (**27**) or a cyclic phosphate (**28**) eliminated P2Y₁₃ receptor antagonist effects (data not shown).

3.3. Antagonistic effect of selected pyridoxal phosphate derivatives on ADP-induced IP₃ synthesis in 1321N1 cells expressing hP2Y₁ or hP2Y₁₂ receptors

Three of the most potent analogues were selected for measurement of inhibition of functional responses of other ADP-responding P2Y receptors expressed in 1321N1 astrocytoma cells. The 3-nitro (**10**), the 2-chloro-5-nitro (**12**) and 4-chloro-3-nitro (**13**) analogues were examined as antagonists at P2Y₁ and P2Y₁₂ subtypes. Although the P2Y₁₂ receptor expressed in 1321N1 cells preferentially couples to inhibition of adenylate cyclase through G_{iα}, an effect of stimulation of PLC also occurs at higher agonists concentrations. Thus, 2-methylthio-ADP stimulated PLC in human P2Y₁₂ receptor-expressing 1321N1 cells with an EC₅₀ of 272 ± 25 nM (n = 3).

In concentration–response studies, **10**, **12**, and **13** inhibited PLC responses to 30 nM 2-methylthio-ADP in human P2Y₁ receptor-expressing 1321N1 cells [8], with IC₅₀ values of >10, >10, and 0.245 ± 0.073 μM, respectively. Compounds **10**, **12**, and **13** were inactive (<20% inhibition at 10 μM) as antagonists of human P2Y₁₂ receptor-mediated PLC responses to 300 nM 2-methylthio-ADP in 1321N1 cells.

4. Discussion

The nucleotide derivative AR-C69931MX, a potent P2Y₁₂ receptor antagonist, has been shown to be a non-competitive antagonist of the human P2Y₁₃ receptor [16]. In the search for more selective P2Y₁₃ receptor antagonists, we first tried the known adenine-based antagonists of P2Y₁ and P2Y₁₂ receptors, MRS2298 (2-[2-(2-chloro-6-methylaminopurin-9-yl)-methyl]propane-1,3-bisoxo(diammoniumphosphate)) and MRS2395 (2,2-dimethyl-propionic acid 3-(2-chloro-6-methylaminopurin-9-yl)-2-(2,2-dimethyl-propionylloxymethyl)-propyl ester), respectively. Neither compound at 10 μM inhibited P2Y₁₃ functional responses under the conditions used in Table 1 (data not shown). Thus, we focused attention on nonnucleoside derivatives. In a previous work the pyridine derivative PPADS has been described as a low potency antagonist for the P2Y₁₃ receptor [14], providing thus a structural lead for the design of new antagonists for this receptor. In the present study a series of novel PPADS analogues was designed and their inhibitory effect was tested on the ADP-induced PLC activity in the hP2Y₁₃-1321N1-Gα₁₆ cells. The most potent antagonists among this series were two compounds containing both chloro and the *m*-nitro group in the phenylazo ring: 2-chloro-5-nitro (**12**, MRS 2211) and 4-chloro-3-nitro (**13**, MRS 2603). The inhibition by these compounds of the ADP (100 nM)-induced inositol trisphosphate synthesis was already evident at high nanomolar concentrations. Compounds **12** and **13** were 45- and 74-fold, respectively, more potent at the P2Y₁₃ receptor than the parental compound PPADS. The interaction of MRS 2211 with the P2Y₁₃ receptor had a competitive character with a pA₂ value of 6.3, calculated from the Schild plot.

Site-directed mutagenesis of P2Y₁ and P2Y₂ receptors has suggested that a cluster of positively charged amino acids within the exofacial side of the transmembrane regions (TM) 6 and 7 might be important in the ligand binding process [2]. A study of the binding of PPADS (negatively charged on the phenyl moiety) and MRS 2210 **4** (having a neutral phenyl moiety) to mutant human P2Y₁ receptors revealed the importance of the positively charged Lys280 of TM6 for both antagonists [8]. Thus, this position of TM6 likely interacts with the 5'-phosphate moiety. The P2Y₁₃ receptor has a positively charged Arg at this position, suggesting that by homology it may serve as a counter-ion for the phosphate moiety. At the P2Y₁₃ receptor, as with the P2Y₁ receptor, neutral phenylazo groups, e.g. **3–9**, displayed considerable potency. Therefore, it seems that the negatively charged substituents on the pyridoxal moiety rather than on the phenylazo group are important in the interaction with the receptor. The *m*-substituted analogues seemed to fit favourably in the receptor site; several *m*-nitro-substituted compounds (**10**, **12**, and **13**, but not **16**) revealed significantly higher potency than analogues with the *m*-sulfonate group (e.g. **11**). Comparison of **11** with the corresponding

methylenephosphonate derivative **19** revealed no effect on affinity.

The question of irreversible binding to the P2Y₁₃ receptor, as a consequence of the aldehyde group of these pyridoxal phosphate derivatives forming a Schiff base with the receptor protein [4,15], as has been proposed to occur at P2X receptors, has not been explored experimentally in this study. However, since the Schild plot demonstrated a slope of approximately 1, the binding appeared to be competitive. Although the aldehyde group is essential for interaction with the P2Y₁₃ receptor, there is no indication that this is due to formation of a covalent bond with the receptor. Similar results were obtained with the P2Y₁ receptor [8].

Recently, it was reported that ADP acting on P2Y₁₃ receptors provides a negative feedback pathway to suppress ATP release from human blood erythrocytes [19], which normally occurs in response to low O₂ levels. Thus, a P2Y₁₃ receptor antagonist might increase ATP release. The receptor is also thought to have a role in the nervous and immune systems [14]. The rat homologue of the receptor was recently cloned and found to have a unique agonist activation profile [20]. With increasing interest in the biological role of the P2Y₁₃ receptor, effective antagonist probes need to be developed for pharmacological characterization.

Selectivity of these pyridoxal phosphate derivatives within the P2 receptor family requires further studies. PPADS and certain analogues have been shown to potently inhibit P2X₁ and P2X₃ ATP-gated ion channels and also, with lower potency, P2X₂, P2X₅, P2Y₁, and P2Y₆ receptors [16,21]. Nevertheless, PPADS is inactive as an antagonist at the P2Y₁₁ and P2Y₁₂ receptors. Thus, these derivatives used as P2Y₁₃ receptor antagonists are expected to avoid the problem associated with use of the nucleotide AR-C67085MX [14], i.e. cross-reactivity with the P2Y₁₁ (as agonist) and P2Y₁₂ (as antagonist) receptors. Indeed, **12** displayed >20-fold selectivity as antagonist of the human P2Y₁₃ receptor in comparison to human P2Y₁ and P2Y₁₂ receptors, and **10** was similarly selective for the P2Y₁₃ receptor. Compound **13** was inactive at the P2Y₁₂ receptor, but did not discriminate between P2Y₁ and P2Y₁₃ receptors. Antagonism of P2X receptors was not evaluated in the present study. Inhibition of ectonucleotidases by related PPADS analogues at high μ M concentrations has been studied [23].

In conclusion, the structure activity relationship of PPADS analogues as antagonists for the human P2Y₁₃ receptor suggests that both *m*-nitro and chloro substitution of the 6-phenylazo ring provides a promising new lead for further improvement of potency and selectivity.

Acknowledgements

The research of K.S. was supported by the Marie Curie Fellowship of the European Community Programme

Human Potential, under contract number HPMF-CT-2001-01472. The authors are solely responsible for the information published, and the European Community is not responsible for any views or results expressed. This work was supported by an Action de Recherche Concertée of the Communauté Française de Belgique and by a grant of the FRSM. The authors are grateful to Mrs. Nicole Vandebosch for technical assistance. We thank Dr. Victor Livengood (NIDDK) for mass spectral measurements. We thank Prof. T. K. Harden for the gift of P2Y₁ receptor-expressing 1321N1 astrocytoma cells. Dr. Yong-Chul Kim was supported by a grant CBM2-B114-001-1-0-0 from the Center for Biological Modulators of the 21st Century Frontier R&D Program, the Ministry of Science and Technology, Korea.

References

- [1] Sak K, Webb TE. A retrospective of recombinant P2Y receptor subtypes and their pharmacology. *Arch Biochem Pharmacol* 2002; 397:131–6.
- [2] Abbracchio MP, Boeynaems J-M, Barnard EA, Boyer JL, Kennedy C, Miras-Portugal MT, et al. Characterization of the UDP-glucose receptor (re-named here the P2Y₁₄ receptor) adds diversity to the P2Y receptor family. *Trends Pharmacol Sci* 2003;24:52–5.
- [3] Costanzi S, Mamedova L, Gao ZG, Jacobson KA. Architecture of P2Y nucleotide receptors: structural comparison based on sequence analysis, mutagenesis, and homology modeling. *J Med Chem* 2004;47: 5393–404.
- [4] Lambrecht G. Agonists and antagonists acting at P2X receptors: selectivity profiles and functional implications. *Naunyn-Schmiedeberg's Arch Pharmacol* 2000;362:340–50.
- [5] Boarder MR, Hourani SMO. The regulation of vascular function by P2 receptors: multiple sites and multiple receptors. *Trends Pharmacol Sci* 1998;9:99–107.
- [6] von Kügelgen I, Wetter A. Molecular pharmacology of P2Y-receptors. *Naunyn-Schmiedeberg's Arch Pharmacol* 2000;362:310–23.
- [7] Kim Y-C, Camaioni E, Ziganshin AU, Ji X-d, King BF, Wildman SS, et al. Synthesis and structure–activity relationships of pyridoxal-6-aryloxy-5'-phosphate and phosphonate derivatives as P2 receptor antagonists. *Drug Dev Res* 1998;45:52–66.
- [8] Guo D, von Kügelgen I, Moro S, Kim Y-C, Jacobson KA. Evidence for the recognition of non-nucleotide antagonists within the transmembrane domains of the human P2Y₁ receptor. *Drug Dev Res* 2002; 57:173–81.
- [9] Unterberger U, Moskvina E, Scholze T, Freissmuth M, Boehm S. Inhibition of adenylyl cyclase by neuronal P2Y receptors. *Br J Pharmacol* 2002;135:673–84.
- [10] Takasaki J, Kamohara M, Saito T, Matsumoto M, Matsumoto S-I, Ohishi T, et al. Molecular cloning of the platelet P2T_{AC} ADP receptor: pharmacological comparison with another ADP receptor, the P2Y₁ receptor. *Mol Pharmacol* 2001;60:432–9.
- [11] Czajkowski R, Lei L, Sabala P, Baranska J. ADP-evoked phospholipase C stimulation and adenylyl cyclase inhibition in glioma C6 cells occur through two distinct nucleotide receptors, P2Y₁ and P2Y₁₂. *FEBS Lett* 2002;513:179–83.
- [12] Communi D, Gonzalez NS, Detheux M, Brezillon S, Lannoy V, Parmentier M, et al. Identification of a novel human ADP receptor coupled to Gi. *J Biol Chem* 2001;276:41479–85.
- [13] Zhang FL, Luo L, Gustafson E, Palmer K, Qiao X, Fan X, et al. P2Y₁₃: identification and characterization of a novel G α_i -coupled ADP

- receptor from human and mouse. *J Pharmacol Exp Ther* 2002;301:705–13.
- [14] Marteau F, Le Poul E, Communi D, Communi D, Labouret C, Savi P, et al. Pharmacological characterization of the human P2Y₁₃ receptor. *Mol Pharmacol* 2003;64:104–12.
- [15] Kim Y-C, Brown SG, Harden TK, Boyer JL, Dubyak G, King BF, et al. Structure activity relationships of pyridoxal phosphate derivatives as potent and selective antagonists of P2X₁ receptors. *J Med Chem* 2001;44:340–9.
- [16] Brown SG, Kim Y-C, Kim S-A, Jacobson KA, Burnstock G, King BF. Actions of a series of PPADS analogues at P2X₁ and P2X₃ receptors. *Drug Dev Res* 2001;53:281–91.
- [17] Kim Y-C, Jacobson KA. Versatile synthesis of 6-alkyl and aryl substituted pyridoxal derivatives. *Synthesis* 2000;119–22.
- [18] Communi D, Pirotton S, Parmentier M, Boeynaems J-M. Cloning and functional expression of a human uridine receptor. *J Biol Chem* 1995;270:30849–52.
- [19] Wang L, Olivecrona G, Gotberg M, Olsson ML, Winzell MS, Erlinge D. ADP acting on P2Y₁₃ receptors is a negative feedback pathway for ATP release from human red blood cells. *Circ Res* 2005;96:189–96.
- [20] Fumagalli M, Trincavelli L, Lecca D, Martini C, Ciana P, Abbracchio MP. Cloning, pharmacological characterisation and distribution of the rat G-protein-coupled P2Y₁₃ receptor. *Biochem Pharmacol* 2004;68:113–24.
- [21] Jacobson KA, King BF, Burnstock G. Pharmacological characterization of P2 (nucleotide) receptors. *Cell Transmissions* 2000;16:3–16.
- [22] Kostenis E. Is Galph_{a16} the optimal tool for fishing ligands of orphan G-protein-coupled receptors?. *Trends Pharmacol Sci* 2001;22:560–4.
- [23] Hoffmann CA, Heine P, Pradel G, Kim Y-C, Jacobson KA, Zimmermann H. Inhibition of ecto-apyrase and ecto-ATPase by pyridoxal phosphate-related compounds. *Drug Dev Res* 2000;51:153–8.